Thermally Tunable Dual Emission of the d^8-d^8 Dimer $[Pt_2(\mu\text{-}P_2O_5(BF_2)_2)_4]^{4-}$

Thomas Hofbeck,[a] Yan Choi Lam,[b] Martin Kalbáč,[c] Stanislav Záliš,[c] Antonín Vlček, Jr.,*[,c,d] and Hartmut Yersin,*[,a]

[a] Universität Regensburg, Institut für Physikalische und Theoretische Chemie, Universitätstrasse 31, D-93040 Regensburg, Germany
[b] Beckman Institute, California Institute of Technology, Pasadena, CA 91125, USA
[c] J. Heyrovský Institute of Physical Chemistry, Academy of Sciences of the Czech Republic, Dolejškova 3, CZ-182 23 Prague, Czech Republic
[d] Queen Mary University of London, School of Biological and Chemical Sciences, Mile End Road, London E1 4NS, United Kingdom

E-mail: hartmut.yersin@ur.de, a.vlcek@qmul.ac.uk

SUPPORTING INFORMATION

Table S1. Temperature-dependence of the fluorescence and phosphorescence quantum yields of Pt(pop-BF_2) (powder). Relative intensities were obtained from the emission spectra and calibrated against measurements in an integrating sphere at 77 K and 298 K.

Temperature / K	Φ(Fluorescence)	Φ (Phosphorescence)	Φ (total)
310	0.126	0.838	0.964
300	0.152	0.811	0.964
290	0.182	0.78	0.962
280	0.212	0.745	0.957
270	0.245	0.71	0.955
260	0.287	0.679	0.966
250	0.321	0.628	0.949
240	0.363	0.591	0.955
230	0.41	0.55	0.959
220	0.45	0.507	0.957
210	0.501	0.463	0.963
200	0.546	0.422	0.968
190	0.584	0.372	0.956
180	0.637	0.338	0.976
170	0.684	0.304	0.988
160	0.719	0.265	0.984
150	0.76	0.238	0.998
140	0.795	0.207	1.002
130	0.815	0.181	0.996
120	0.835	0.158	0.993
110	0.851	0.139	0.99
100	0.875	0.125	1
90	0.881	0.112	0.994
80	0.887	0.102	0.989
70	0.894	0.091	0.985
60	0.893	0.081	0.974
50	0.898	0.075	0.973
40	0.89	0.07	0.96
30	0.894	0.068	0.961
20	0.891	0.067	0.958
15	0.889	0.066	0.956
10	0.891	0.066	0.957
8	0.89	0.065	0.955
7	0.885	0.064	0.949
6.5	0.885	0.064	0.949
6	0.88	0.063	0.944
5	0.88	0.063	0.943
4	0.88	0.062	0.943
2.5	0.882	0.062	0.944
1.5	0.885	0.063	0.948

Table S2. Spectroscopically and photophysically relevant spin-orbit electronic transitions of Pt(pop-BF_2). Symmetry labeling corresponds to idealized C_{2h} symmetry. (Spin-orbit D_{4h} labels in parenthesis.) Calculation: SO-TDDFT (COSMO-MeCN). Adapted from ref. 1.

SO state	Contributions of spin – free states	Character	Energy (cm^{-1})	Oscillator strength
aA_u (aA_{1u})	a^3A_u (98%) + c^3B_u (0.8%) + d^3B_u (0.9%) + b^3B_u (0.3%)	dσ*→pσ	20278	0
aB_u (aE_u)	a^3A_u (98%) + d^1B_u (0.7%) + c^3B_u (0.9%) + b^3B_u (0.3%)	dσ*→pσ	20332	0.00026
bB_u (aE_u)	a^3A_u (98%) + f^1B_u (0.5%) + a^1B_u (0.2%) + b^3B_u (0.9%)	dσ*→pσ	20338	0.00017
bA_u (aA_{2u})	a^1A_u (95.6%) + c^3B_u (1.4%) + d^3B_u (1.4%) + a^3B_u (0.9%) + b^3B_u (0.6%)	dσ*→pσ	27244	0.230
cA_u (bE_u)	a^3B_u (50%) + b^3B_u (50%)	LMMCT pπ→pσ	33076	0.000
dA_u (bE_u)	a^3B_u (50%) + b^3B_u (50%)	LMMCT pπ→pσ	33076	0.000
aA_g (cE_u)	a^3B_g (50%) + b^3B_g (50%)	LMMCT	33304	0.000
bA_g (cE_u)	a^3B_g (50%) + b^3B_g (50%)	LMMCT	33314	0.000
cB_u (dE_u)	a^3B_u (89%) + b^1B_u (11%)	LMMCT pπ→pσ	33788	0.002
dB_u (dE_u)	b^3B_u (89%) + a^1B_u (11%)	LMMCT pπ→pσ	33855	0.001
eA_u (bA_{2u})	b^3B_u (51%) + b^3B_u (49%) + a^1A_u (2%)	LMMCT pπ→pσ	35468	0.003
cA_g (E_g)	c^3B_g(40%) + d^3B_g(52%) + c^1A_g(3%)	dπ*→pσ LMMCT	36746	0.000
dA_g (E_g)	b^3A_g (24%) + d^3B_g(60%) + c^1A_g(10%)	dπ*→pσ LMMCT	36812	0.000
aB_g (E_g)	c^3B_g(41%) + d^3B_g(50%)	dπ*→pσ LMMCT	36945	0.000
cB_u (eE_u)	a^1B_u (86%) + b^3B_u (13%)	LMMCT pπ→pσ	37184	0.012
dB_u (eE_u)	b^1B_u (86%) + a^3A_u (13%)	LMMCT	37194	0.009
fA_u (cA_{2u})	a^3B_u (49%) + b^3B_u (50%) + a^1A_u (1%)	LMMCT pπ→pσ	43276	0.003
eB_u (fE_u)	d^3B_u (80%) + d^1B_u (20%)	LMMCT	43561	0.007
fB_u (fE_u)	c^1B_u (98%)	LMMCT	45624	0.005
gB_u(gE_u)	Mixed	LMMCT	45660	0.006
hB_u (hE_u)	d^1B_u (78%) + c^3B_u (18%) + a^1B_u (2%)	dπ→pσ LMMCT	47236	0.028
iB_u (gE_u)	e^1B_u (67%) + e^1B_u (28%)	LMMCT	47587	0.007
jB_u (hE_u)	f^1B_u (58%) + d^3B_u (33%)	LMMCT dπ→pσ	47677	0.016

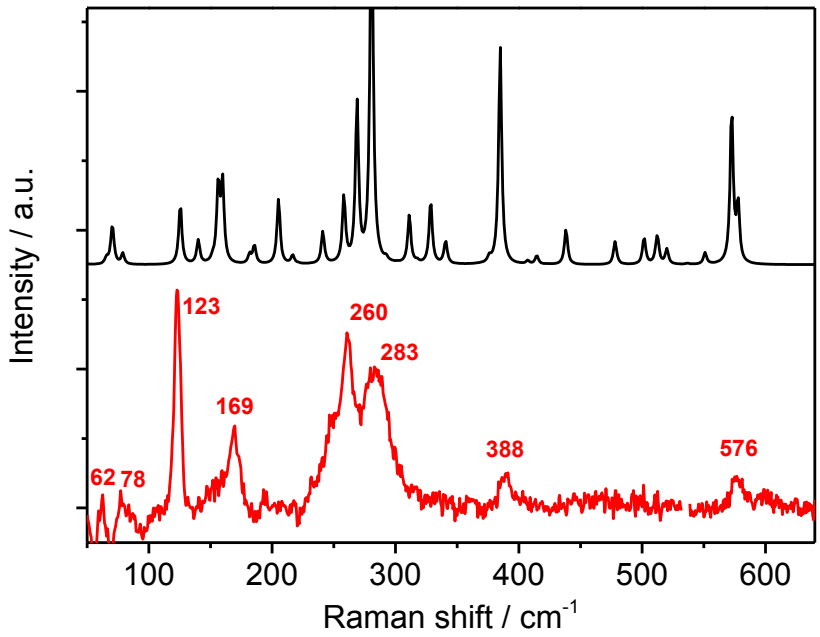

Figure S1. Raman spectra of $[Bu_4N]_4[Pt(pop\text{-}BF_2)]$. Bottom-red: experimental spectrum measured on a solid sample (λ_{exc} = 1064 nm). Top-black: DFT-calculated spectrum (PBE0, vacuum).

Table S3. Selected experimental and DFT calculated (C_{2h} symmetry) Raman-active vibrations of Pt(pop-BF_2).

Wavenumber cm^{-1}		Raman activity $Å^4Amu^{-1}$		Symmetry[a]	
Expt.	Calc'd	(calc'd)	Assignment	C_{2h}	D_{4h}
	22	0.2	BF_2 swing	A_g	A_{1g}
	30	0.2	BF_2 swing	A_g	A_{1g}
	40	0.2	BF_2 swing	A_g	A_{1g}
~62	58	0.2	pop-BF_2 deformation	B_g	A_{1g}
	65	1.0	pop-BF_2 deformation	A_g	E_g
~78	69	1.2	pop-BF_2 deformation	B_g	E_g
	75	0.5	pop-BF_2 deformation	A_g	A_{1g}
123	124	3	ν(Pt-Pt)	A_g	A_{1g}
	139	1.2	pop-BF_2 torsion	B_g	B_{1g}
	150	0.2	pop-BF_2 breathing	B_g	E_g
169	154	4	pop-BF_2 breathing + ν(Pt-Pt)	A_g	E_g
	159	4	pop-BF_2 breathing + ν(Pt-Pt)	A_g	E_g
~194	186	1	pop-BF_2 deformation	B_g	E_g
	204	3	ν(Pt-Pt)	A_g	A_{1g}
	214 or 219	0	skeletal def.	B_g	A_{2g}
~248	254	4	δ(P-O-P) + ν(Pt-P) + skeletal def.	B_g	B_{1g}
260	269	7	δ(P-O-P) + ν(Pt-P) + skeletal def.	A_g	A_{1g}
283	280	22	ν(Pt-P) + δ(P-O-P) + skeletal def.	A_g	A_{1g}
	327	3	skeletal def.	A_g	-
388	383	10	δ(P-O-P)	A_g	A_{1g}
576	571	8	δ(P-O-B)+ δ(O-B-O)	A_g	A_{1g}
	576	3	δ(P-O-B)+ δ(O-B-O)	A_g	-
	670	3	δ(P-O-B)+ δ(O-B-O)	A_g	E_g
	713	3	δ(P-O-P)+ δ(O-B-O)	A_g	A_{1g}
	810	20	ν(Pt-P)+ δ(P-O-P)	A_g	A_{1g}
	819	3	ν(B-O)+ ν(P-O)	A_g	-
	841	0	ν(B-O)+ ν(P-O)	B_g	A_{2g}
	961	1	ν(P-O) + ν(B-O) + skeletal def.	A_g	E_g
	961	2	ν(P-O) + ν(B-O) + skeletal def.	B_g	E_g
	1048	12	ν(B-O) +δ(P-O-P)	A_g	A_{1g}
1112	1107	5	ν(P-O)	B_g	E_g
	1120	12	ν(P-O)	A_g	E_g
	1131	7	ν(B-F)+ ν(P-O)	A_g	B_{2g}
1150	1151	3	ν(B-F)	A_g	B_{2g}
	1156	9	ν(B-F)	A_g	A_{1g}
	1175	10	ν(B-F)	A_g	A_{1g}

[a] Left column: symmetry of vibrational modes obtained for the lowest-energy C_{2h} structure. Right column: symmetry of vibrational modes in a D_{4h} point group.

Table S4. Fluorescence lifetime and quantum yield of microcrystalline Pt(pop-BF_2) as a function of temperature. The radiative ($k_r = \phi_{fl} / \tau_{fl}$) and non-radiative ($k_{nr} = (1 - \phi_{fl}) / \tau_{fl}$) decay rates were calculated from these quantities.

Temperature [K]	τ_{fl} [ns]	Φ(Fluorescence)	k_r [10^8 s^{-1}]	k_{nr} [10^8 s^{-1}]
5	3.22	0.88	2.73	0.372
10	3.22	0.89	2.77	0.338
30	3.22	0.89	2.78	0.329
40	3.22	0.89	2.76	0.342
50	3.20	0.90	2.81	0.319
60	3.17	0.89	2.81	0.337
70	3.16	0.89	2.83	0.336
80	3.13	0.89	2.83	0.361
90	3.11	0.88	2.83	0.382
100	3.10	0.88	2.82	0.403
110	3.09	0.85	2.75	0.482
120	3.07	0.84	2.72	0.538
130	3.04	0.82	2.68	0.608
140	3.00	0.80	2.65	0.683
150	2.96	0.76	2.57	0.811
160	2.91	0.72	2.47	0.965
170	2.84	0.68	2.41	1.11
180	2.72	0.64	2.34	1.33
190	2.62	0.58	2.23	1.59
200	2.49	0.55	2.19	1.82
210	2.35	0.50	2.13	2.12
220	2.20	0.45	2.05	2.50
230	2.05	0.41	2.00	2.88
240	1.91	0.36	1.90	3.34
250	1.73	0.32	1.85	3.92
260	1.57	0.29	1.82	4.53
270	1.40	0.25	1.75	5.40
280	1.23	0.21	1.73	6.41
290	1.09	0.18	1.68	7.53
300	0.95	0.15	1.60	8.95
310	0.83	0.13	1.51	10.5

Raman spectroscopy - Experimental.

The spectra were measured on Labram HR Raman spectrometer (Horiba Jobin-Yvon) with a resolution of about 1 cm^{-1}, excited with a 1064 nm laser. The spectrometer was interfaced to a microscope (Olympus, objective 50x). The size of the laser spot was about 1 micrometer. A solid powder sample was placed in a flat 2 mm quartz cell under dry argon atmosphere. Raman bands due to the Bu_4N^+ counter cation were identified by a separate measurement on $[Bu_4N]I$ powder, performed at identical conditions.

DFT Calculations

The electronic structures of the Pt(pop-BF_2) and Pt(pop) complex anions were calculated by density functional theory (DFT) methods using the Gaussian 09[2] program package. Calculations employed the hybrid Perdew, Burke and Ernzerhof[3,4] (PBE0) exchange and correlation functional or the functional including Becke's gradient correction[5] to the local exchange expression in conjunction with Perdew's gradient correction[6] to the local correlation (BP86). For H, B, P, O and F atoms, 6-311g(3d) polarized triple - ζ basis sets,[7] together with quasi-relativistic small core effective core pseudopotentials and the corresponding optimized set of basis functions for Pt.[8,9] Geometry optimization was followed by vibrational analysis; no imaginary frequencies were found for energy minimum of the C_{2h} conformer shown in Figure 1-main text, whose structure matches the experimental one. (No true energy minima were obtained for C_{4h} and D_{4h} conformers.) The calculated bond lengths agree very well with the experimental values and reproduce the subtle structural changes between Pt(pop) and Pt(pop-BF_2), validating the calculation (Table S5). The match is better for the hybrid functional PBE0 than for the pure functional BP86 that slightly overestimates the bond lengths.

Table S5. Experimental and DFT-calculated bond lengths for Pt(pop-BF_2) and Pt(pop).

Bond	Exp.	Calc. PBE0	Calc. BP86
$[Ph_4As]_4[Pt_2(pop\text{-}BF_2)_4]$[1]			
Pt-Pt	2.8895(1)	2.901	2.922
Pt-P (average)	2.294	2.302	2.324
P-O(-P) (average)	1.614	1.628	1.656
$K_4[Pt_2(pop)_4]$[10,11]			
Pt-Pt	2.925(1)	2.929	2.948
Pt-P (average)	2.321(4)	2.351	2.374
P-O(-P) (average)	1.622(12/14)	1.644	1.674

References

(1) Záliš, S.; Lam, Y. C.; Gray, H. B.; Vlček, A., Jr. *Inorg. Chem.* **2015**, *54*, 3491−3500.
(2) Frisch, M. J.; Trucks, G. W.; Schlegel, H. B.; Scuseria, G. E.; Robb, M. A.; Cheeseman, J. R.; Scalmani, G.; Barone, V.; Mennucci, B.; Petersson, G. A.; Nakatsuji, H.; Caricato, M.; Li, X.; Hratchian, H. P.; Izmaylov, A. F.; Bloino, J.; Zheng, G.; Sonnenberg, J. L.; Hada, M.; Ehara, M.; Toyota, K.; Fukuda, R.; Hasegawa, J.; Ishida, M.; Nakajima, T.; Honda, Y.; Kitao, O.; Nakai, H.; Vreven, T.; Montgomery, J. A., Jr.; Peralta, J. E.; Ogliaro, F.; Bearpark, M.; Heyd, J. J.; Brothers, E.; Kudin, K. N.; Staroverov, V. N.; Kobayashi, R.; Normand, J.; Raghavachari, K.; Rendell, A.; Burant, J. C.; Iyengar, S. S.; Tomasi, J.; Cossi, M.; Rega, N.; Millam, J. M.; Klene, M.; Knox, J. E.; Cross, J. B.; Bakken, V.; Adamo, C.; Jaramillo, J.; Gomperts, R.; Stratmann, R. E.; Yazyev, O.; Austin, A. J.; Cammi, R.; Pomelli, C.; Ochterski, J. W.; Martin, R. L.; Morokuma, K.; Zakrzewski, V. G.; Voth, G. A.; Salvador, P.; Dannenberg, J. J.; Dapprich, S.; Daniels, A. D.; Farkas, O.; Foresman, J. B.; Ortiz, J. V.; Cioslowski, J.; Fox, D. J.; Gaussian 09, Revision C.01, Gaussian, Inc.: Wallingford CT, 2009.
(3) Perdew, J. P.; Burke, K.; Ernzerhof, M. *Phys. Rev. Lett.* **1996**, *77*, 3865-3868.
(4) Adamo, C.; Scuseria, G. E.; Barone, V. *J. Chem. Phys.* **1999**, *111*, 2889-2899.
(5) Becke, A. D. *Phys. Rev. A* **1988**, *38*, 3098.
(6) Perdew, J. P. *Phys. Rev. A* **1986**, *33*, 8822.
(7) Raghavachari, K.; Binkley, J. S.; Seeger, R.; Pople, J. A. *J. Chem. Phys.* **1980**, *72*, 650-654.
(8) Andrae, D.; Häussermann, U.; Dolg, M.; Stoll, H.; Preuss, H. *Theor. Chim. Acta* **1990**, *77*, 123-141.
(9) Martin, J. M. L.; Sundermann, A. *J. Chem. Phys.* **2001**, *114*, 3408.
(10) Dos Remedios Pinto, M. A.; Sadler, P. J.; Neidle, S.; Sanderson, M. R.; Subbiah, A.; R., K. *J. Chem. Soc., Chem. Comm.* **1980**, 13-15.
(11) Marsh, R. E.; Herbstein, F. H. *Acta Crystallogr., Sect. B* **1983**, *39*, 280-287.